Augmentation of Apoptosis and Tumor Regression by Flavopiridol in the Presence of CPT-11 in Hct116 Colon Cancer Monolayers and Xenografts[1]

Monica Motwani, Christoph Jung, Francis M. Sirotnak, Yuhong She, Manish A. Shah, Mithat Gonen, and Gary K. Schwartz[2]

Gastrointestinal Oncology Research Laboratory, Division of Solid Tumor Oncology, Department of Medicine [M. M., C. J., M. A. S., G. K. S.], Program of Molecular Pharmacology and Experimental Therapeutics [F. M. S., Y. S.], and Department of Epidemiology and Biostatistics [M. G.], Memorial Sloan Kettering Cancer Center, New York, New York 10021

ABSTRACT

CPT-11, a DNA topoisomerase I inhibitor, has demonstrated clinical activity in colorectal cancer. Flavopiridol, a cyclin-dependent kinase inhibitor, is rapidly emerging as a chemotherapy modulator. To enhance the therapeutic index of CPT-11 in colon cancer, we studied the combination of these two drugs in relatively resistant human colon cancer cells, Hct116. Exposure of parental Hct116 cells to clinically achievable concentrations of SN-38 (the active metabolite of CPT-11) induces p21 and a G_2 arrest. However, these conditions fail to induce apoptosis. In contrast, Hct116 cells that are p21 deficient (p21−/− Hct116) readily undergo apoptosis after treatment with SN-38. In this study we show that the parental Hct116 cells can be sensitized to undergo apoptosis by the addition of flavopiridol after SN-38 treatment. The induction of apoptosis was greatest with sequential therapy consisting of SN-38 followed by flavopiridol. Clonogenic assays also showed greatest inhibition with this sequence. Sequential treatment with SN-38 followed by flavopiridol was associated with higher activation of caspase-3 and greater cleavage of both p21 and XIAP, an inhibitor of apoptosis, compared with other treatment schedules. CPT-11 induced some tumor regressions but no complete responses in the p21-intact Hct116 xenografts. CPT-11 with flavopiridol more than doubled tumor regression, compared with CPT-11 alone, and produced a 30% complete response rate. Our studies indicate that CPT-11 induces cell cycle arrest rather than cell death and that flavopiridol, by activating the caspase cascade, cleaves the inhibitors of apoptosis and sensitizes the cells to undergo cell death. Thus, flavopiridol combined with CPT-11 may provide a completely new therapeutic approach in the treatment of colon cancer.

INTRODUCTION

One of the major factors that can influence resistance to DNA-damaging agents is the balance between damage (or stress) and repair. In response to DNA damage, checkpoints are alerted in checkpoint-intact cells. This results in cell cycle arrest and initiation of DNA repair (1). However, if the damage (or stress) is beyond the capability of cell to repair, then apoptosis is induced (2, 3). Thus, a protective mechanism has been established by which checkpoint-intact cells initiate cell cycle arrest and induce a repair mechanism that protects the cell from the cytotoxic effects of DNA-damaging agents. In essence, this mechanism of self-repair prevents chemotherapy-induced apoptosis. We suspect that this plays a major role in the general failure of many conventional chemotherapeutic agents. Thus, the ability to reverse this process by agents that in themselves modulate the cell cycle would constitute a major advance in cancer therapy.

The camptothecin CPT-11 is a topoisomerase I inhibitor that induces DNA damage and transient S-phase arrest (4, 5). Increased sensitivity to this agent has been observed in cells with defective checkpoints that prevent the cells from arresting in G_2 after drug exposure (6). Thus, the relative sensitivity of tumor cells to CPT-11 appears to depend, at least in part, on the absence or presence of intact checkpoints within the cell cycle.

It has been hypothesized that the damage by radiation or chemotherapy at physiological conditions does not induce sufficient stress to induce cell death. To enhance the therapeutic index, combinations of various drugs have been used in cancer therapy. For example, a synergy is observed when DC3F cells are treated with ionizing radiation and CPT-11 in a sequential manner (7). It has been suggested that "sublethal" DNA damage of CPT-11 is converted into lethal damage by radiation-induced DNA damage. A similar phenomenon has been observed when CPT-11 is combined with 5-fluorouracil (8). All of these studies have included the combination of conventional chemotherapeutic agents or radiation.

Flavopiridol, a CDK[3] inhibitor, has been reported to bind to DNA and induce DNA damage (9). Furthermore, it has been

Received 12/29/00; revised 8/2/01; accepted 8/10/01.
The costs of publication of this article were defrayed in part by the payment of page charges. This article must therefore be hereby marked *advertisement* in accordance with 18 U.S.C. Section 1734 solely to indicate this fact.
[1] This work was supported by Grant R01CA67819 from the National Cancer Institute.
[2] To whom requests for reprints should be addressed, at Memorial Sloan Kettering Cancer Center, 1275 York Avenue, New York, NY 10021. Phone: (212) 639-8324; Fax: (212) 717-3320; E-mail: schwartg@mskcc.org.

[3] The abbreviations used are: CDK, cyclin-dependent kinase; CR, complete response; fmk, fluoromethyl ketone; PARP, poly(ADP-ribose) polymerase.

shown that the addition of flavopiridol to other "stress-inducing" agents promotes cytotoxicity and induces apoptosis (10, 11). Therefore, it stands to reason that in checkpoint-intact cells, the addition of flavopiridol to CPT-11 should produce a degree of damage that results in apoptosis rather than cell cycle arrest. In addition, we believe that any effect seen *in vitro* should also produce an enhanced antitumor effect *in vivo* that could not be achieved with CPT-11 or flavopiridol alone. Our studies indicated that the addition of flavopiridol to SN-38-treated Hct116 cells augments the induction of apoptosis and the inhibition of colony formation. Furthermore, the regression of established Hct116 xenografts obtained with CPT-11 was significantly increased with flavopiridol. Moreover, CRs were observed when CPT-11 and flavopiridol were given sequentially and separated by specific time intervals.

MATERIALS AND METHODS

Cell Culture and Drug Treatments for Cell Lines. The p21-intact and -deficient Hct116 human colon cancer cell lines were kindly provided by Dr. Bert Vogelstein (John Hopkins Oncology Center, Baltimore, MD). The cell lines were maintained in RPMI supplemented with 10% heat-inactivated fetal bovine serum, penicillin, and streptomycin at 37°C in 5% carbon dioxide. All cultures were tested as *Mycoplasma* free. The stock solutions of SN-38 (5 mM; supplied by Dr. Patrick McGovren, Pharmacia, Peapack, NJ), fmk-derivatized peptides of caspase-3 inhibitor z-DEVD (z-DEVD-fmk), and pan caspase inhibitor z-VAD (z-VAD-fmk; 50 mM; R&D Systems) were prepared in DMSO, whereas flavopiridol (4.5 mM; graciously supplied by Dr. Edward Sausville, National Cancer Institute, Bethesda, MD) and PS-341 (10 mM; graciously supplied by Louis Grenier, Millenium Pharmaceuticals, Inc., Cambridge, MA) were prepared in water. The stocks were stored at −20°C, and drugs were diluted in the media before use.

Colony Formation Assays. Hct116 cells (8×10^5) were plated, in duplicate, in 60-mm plates and incubated for 24 h to allow cells to adhere. Cells were treated with various doses of SN-38 and flavopiridol alone for 24 h. At the end of treatment, both floating and attached cells were collected by trypsinization and centrifuged for 5 min. Cells were plated in triplicate at the density of 1000 cells/100-mm plate containing 10 ml of drug-free medium and were allowed to grow for 10 days. The resulting colonies were stained with 0.01% crystal violet for 30 min. Control plates usually contained 300–350 colonies. Cells were also treated with various doses of SN-38 and a fixed flavopiridol dose in different schedules: concomitant treatment for 24 h; sequential treatment with SN-38 for 24 h followed by removal of the medium and the addition of medium containing flavopiridol for 24 h; or the two drugs given in reverse sequence. For sequential treatment, the floating cell were collected after treatment with the first drug and added back for treatment with the second drug. At the end of treatment, cells were trypsinized and plated to form colonies as above.

Apoptosis Assays. Measurement of apoptosis by quantitative fluorescence microscopy was performed as described previously (10). The appearance of oligonucleosomal DNA fragmentation characteristic of apoptosis was determined by agarose gel electrophoresis. The cells were treated as above and lysed with 2% SDS containing 10 μg/ml RNase A and incubated at 37°C for 2 h. NaCl (5 M) was added to a final concentration of 1 M, and cells were scraped and stored at 4°C for 2–24 h. The lysed cells were centrifuged for 30 min at 12,000 rpm. DNA unassociated with intact chromatin residing in the supernatant was extracted by phenol-chloroform and precipitated with ethanol. DNA (10 μg) was resolved by agarose gel electrophoresis in 1× Tris-acetate-EDTA for 1 h on 1.5% agarose gel impregnated with ethidium bromide.

MPM-2/Propidium Iodide Bivariate Flow Cytometry. Staining with MPM-2 antibody and propidium iodide was performed as described previously (10). In this method, MPM-2-positive (mitotic) cells show increased green fluorescence and are shifted above the baseline of the dot plot.

Kinase Activity Assay. Cyclin B1/cdc2 kinase assays were performed as described previously (10). In brief, cyclin B1 was immunoprecipitated from 200 μg of lysate prepared from cells treated with various treatment conditions, and the kinase assay was performed with histone H1 as substrate and [γ-^{32}P]ATP as a phosphate donor. The activity levels on autoradiographs were quantified by a densitometric scanning system.

Western Analysis. Western blots were prepared as described previously (10). The membranes were probed with p53, p21 (Santa Cruz Biotechnology), PARP, and caspase-3 (PharMingen), and XIAP (Transduction Laboratories). The primary antibodies were detected with horseradish peroxide secondary antibody (Amersham Life Sciences) and subjected to ECL Chemiluminescence reagents (DuPont NEN Life Science Products, Boston, MA). The levels of expression were quantified by a densitometric scanning system.

Immunoprecipitation of Cyclin/CDK Complexes. Cyclin B1 and E immunoprecipitation was performed as described previously in kinase assays (10). The beads were washed three times with lysis buffer and separated by SDS-PAGE, and Western analysis of bound proteins was performed as described above.

RNA Extraction and Northern Blot Analysis. Total RNA was extracted from cells treated with different schedules of SN-38 and flavopiridol by a described previously cesium chloride method (12). Twenty μg of total RNA were electrophoresed on a 1% agarose-phosphate buffer gel and blotted onto Hybond-N nylon membranes (Amersham); the RNA was then cross-linked by UV Stratalinker (Stratagene). The membranes were hybridized with ^{32}P-labeled p21 full-length cDNA probe (a gift from Dr. David Beach, Howard Hughes Medical Institute, Cold Spring Harbor Laboratories, Cold Spring Harbor, NY) in Expresshyb hybridization solution (Clontech, Palo Alto, CA). The probe was labeled previously by random priming [^{32}P]dCTP incorporation using a random-prime labeling kit (Amersham). The probe was purified by passing through Sephadex Quick Spin column (Boehringer Mannheim).

Nuclear Run-On Assays. Nuclei were obtained, and assays were performed by a modification of previously described procedures (12). Briefly, 5×10^7 cells from each treatment condition were lysed in 2 ml of NP40 buffer [10 mM Tris (pH 7.4), 10 mM NaCl, 3 mM $MgCl_2$, 0.5% NP40], and nuclei were harvested, resuspended in 110 μl of glycerol storage buffer [40% glycerol, 10 mM Tris (pH 7.4), 80 mM KCl, 5 mM $MgCl_2$, 0.1 mM EDTA], and stored at −80°C. Forty μl of nuclear run-on

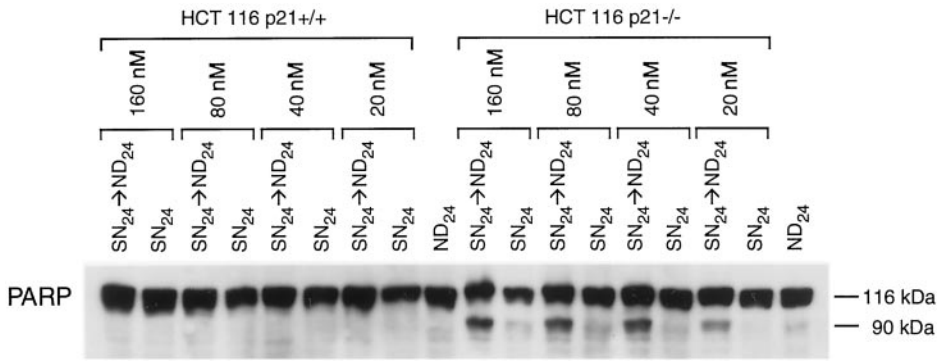

Fig. 1 Differential sensitivity of p21-intact and -deficient Hct116 cells to SN-38: Western blot analysis of PARP cleavage. Cells were treated with varying concentrations of SN-38 for 24 h or SN-38 for 24 h followed by no drug for 24 h, and protein was harvested. Equal loading of protein was verified by staining with Amido black.

buffer [20 mM Tris (pH 8), 0.6 M KCl, 10 mM $MgCl_2$, 2 mM each of ATP, GTP and CTP] and 10 μl of [^{32}P]UTP (3000 Ci/mmol; NEN) were added to the nuclear suspension, and the transcription run-on reaction was allowed to proceed at 30°C for 30 min; the reaction was terminated with 40 μl of stop solution (300 units of DNase I, 1.5 M NaCl, 150 mM $MgCl_2$, and 5 mM $CaCl_2$) at 30°C for 5 min. One μl of proteinase K (20 mg/ml) and 25 μl of buffer [5% SDS, 50 mM EDTA, 100 mM Tris (pH 7.4)] were added and incubated for 30 min at 37°C. The newly formed RNA was extracted as described by Dai *et al.* (13). DNA dot blots with equal quantities of various linearized DNAs were prepared on nylon membranes. The DNA plasmids used included negative control (plasmid PUC), p21 full-length cDNA in pBluescript (a gift from Dr. David Beach), and positive control (a 400-bp fragment of *GAPDH* in pBluescript, isolated during subtraction hybridization in our laboratory). The prehybridization (1 h) and hybridization (18 h) were carried out in ExpressHyb at 65°C. The autoradiograph was obtained after 3 days of exposure of filters at −80°C.

Xenograft Growth Assay. The general procedure used in the experiments has been described previously (14). Athymic-NCr-nu male mice (8–10 weeks of age) were inoculated s.c. in the flank with minced p21-intact Hct116 tumor cells mixed with Matrigel (Becton Dickinson). Treatment was started on the third day after the inoculation of tumor; mice were treated with the maximum tolerated dose of CPT-11 either as a single agent or in combination. The maximum tolerated dose of flavopiridol was used as a single agent and decreased in combination therapy to minimize the cytotoxicity. The average tumor volume at the day of treatment was 27–29 mm^3. Mice received CPT-11 alone (100 mg/kg), flavopiridol alone (11 mg/kg), or CPT-11 (100 mg/kg) followed by flavopiridol (3 mg/kg) 4, 7, 16, or 24 h later. Mice in the control group were given vehicle (PBS) alone. All drugs were administered i.p. twice a week for a total of five injections. Tumors were measured every 3–4 days with calipers, and tumor volumes were calculated by the formula: $4/3 \times \pi \times r^3$, where r = (larger diameter + smaller diameter)/4. The percentage of tumor regression was calculated as the percentage ratio of the difference between baseline and final tumor volume to the baseline volume. Mice showing no palpable tumor 45 days after treatment and mice with small residual tumor nodules that showed no microscopic evidence of residual disease were counted as CR. The percentage of CR was the number of animals with CR divided by the total number of animals treated, multiplied by 100. These studies were performed in accordance with NIH guidelines (15).

Biostatistical Analysis. All *in vitro* experiments were done in duplicate and were repeated at least three times unless otherwise indicated. The statistical significance of the experimental results was determined by the two-sided *t* test. For *in vivo* studies, the area under the time-volume curve was used as a summary measure for each mouse. This area was calculated using the trapezoidal rule. This method takes the longitudinal aspect of the data into account and does not require assumptions of linear growth (or decay), which are clearly violated for our data. Treatment groups were compared in pairs, using the exact permutation distribution of the areas under the curve (16).

RESULTS

G_2 Checkpoint-defective Cells Exhibit Increased Sensitivity to SN-38. It has been shown that p21-deficient Hct116 cells have defective G_1-S and G_2-M checkpoint functions (17). We studied the sensitivity of parental and p21-deficient Hct116 cells to SN-38. The cells were treated with SN-38 (concentrations of 20–160 nM) for 24 h or SN-38 for 24 h followed by 24 h in drug-free medium. As shown in Fig. 1, the p21-intact cell line did not show PARP cleavage, an indicator of caspase activation and apoptosis, at the highest concentration tested (160 nM). In contrast, p21-deficient Hct116 cells, under identical treatment conditions, showed PARP cleavage at SN-38 concentrations as low as 20 nM. This was confirmed by staining of the SN-38 treated parental and p21-deficient cells with 4′,6-diamidino-2-phenylindole, which stains nuclear chromatin. Only the p21-deficient cells showed condensation of nuclei, a hallmark of apoptosis, with SN-38. Other cell lines, including the colon and breast cancer cell lines HT-29 and MDA-MB-468, respectively, which are p53 defective and thus have defective G_1-S and G_2-M checkpoints, were also sensitive to SN-38, as indicated by PARP cleavage and caspase-3 activation at SN-38 concentrations as low as 20 nM (data not shown).

SN-38 Induces Cell Cycle Arrest at G_2 in Hct116 Cells. We examined cell cycle changes after SN-38 treatment in p21-intact and -deficient Hct116 cells. Our results were similar to those obtained by various other investigators with these cell lines in response to DNA-damaging agents, including radiation and etoposide (18, 19). In particular, SN-38 at 20 nM induced transient S-phase arrest in both cell lines. The S-phase popula-

tion increased from 40% to 60% after 15 h of treatment with SN-38 in both cell types. After 24 h of treatment with SN-38, the cells accumulated in the S and G_2 phases, and a significant decrease in the G_1 population was observed (Fig. 2*A*). Twenty-four h after the removal of SN-38 ($SN_{24}\rightarrow ND_{24}$), both cell types accumulated in G_2-M with 4n DNA content. At this stage, a significant difference was observed between the two cell lines. As shown in Fig. 2*A*, p21-intact cells with 4n DNA showed <1% MPM-2 labeling, indicating that cells with 4n DNA content were arrested in G_2. This G_2 arrest was further confirmed by a dramatic decrease in cyclin B1/cdc2 kinase activity in the p21+/+ cells treated with SN-38 followed by no drug (Fig. 2*B*), again indicating G_2 arrest. Although p21-deficient cells with 4n DNA also accumulated after treatment with SN-38 followed by no drug, these cells, in contrast, showed sustained activation of cyclin B1/cdc2 kinase activity (Fig. 2*B*). The MPM-2 labeling of asynchronous p21−/− Hct116 cells after treatment with SN-38 followed by no drug also showed an increase in cells in mitosis (5%; Fig. 2*A*).

Flavopiridol Sensitizes SN-38-treated Cells and Induces Apoptosis. We examined the combination of flavopiridol and SN-38 administered both concurrently and sequentially in the relatively SN-38-resistant p21-intact Hct116 cells. The cells were treated with 20 nM SN-38 and 150 nM flavopiridol in four separate schedules: individually, concurrently and sequentially with SN-38 for 24 h followed by flavopiridol for 24 h, or the same drugs given in reverse sequence. SN-38 for 24 h (SN_{24}) or SN-38 for 24 h followed by no drug for 24 h ($SN_{24}\rightarrow ND_{24}$) resulted in only 1% apoptosis. Flavopiridol for 24 h (F_{24}) induced 12 ± 1% apoptosis. Sequential treatment of Hct116 cells with SN-38 for 24 h followed by flavopiridol for 24 h ($SN_{24}\rightarrow F_{24}$) showed the highest induction of apoptosis (43 ± 0.5%; $SN_{24}\rightarrow F_{24}$ *versus* $SN_{24}\rightarrow ND_{24}$, $P < 0.005$). The pretreatment of cells with flavopiridol ($F_{24}\rightarrow SN_{24}$) resulted in only an additive effect (15 ± 2%) compared with SN-38 or flavopiridol alone. Concomitant therapy [$(SN+F)_{24}$] induced apoptosis in 30 ± 2% of the treated cells. The percentage of induction of apoptosis with $SN_{24}\rightarrow F_{24}$ was significantly greater than that obtained with either the reverse sequence ($SN_{24}\rightarrow F_{24}$ *versus* $F_{24}\rightarrow SN_{24}$, $P < 0.001$) or concomitant therapy [$SN_{24}\rightarrow F_{24}$ *versus* $(SN+F)_{24}$, $P < 0.05$].

Gel electrophoretic analysis of DNA obtained from cells treated with various schedules of SN-38 and flavopiridol revealed more intense oligonucleosomal bands in cells treated with $SN_{24}\rightarrow F_{24}$ compared with those treated with other drug schedules (Fig. 3*A*). In keeping with these observations, higher activation of caspase-3 (*i.e.*, formation of 24-, 20-, and 17-kDa forms) was observed in cells treated with $SN_{24}\rightarrow F_{24}$ compared with those with other treatment schedules (Fig. 3*B*). Cells treated with a combination of SN-38 and flavopiridol together for 24 h [$(SN+F)_{24}$] also showed significant activation of caspase-3, albeit to a lesser degree, when compared with cells treated with $SN_{24}\rightarrow F_{24}$. PARP, the 116-kDa caspase-3 substrate, was completely degraded into its 90-kDa cleaved product in cells treated sequentially with SN-38 followed by flavopiridol, further supporting the greater induction of apoptosis in this treatment schedule. In general, the trend was $SN_{24}\rightarrow F_{24} > (SN+F)_{24} > F_{24}$ for the percentage of induction of apoptosis, caspase-3 activation, and PARP cleavage.

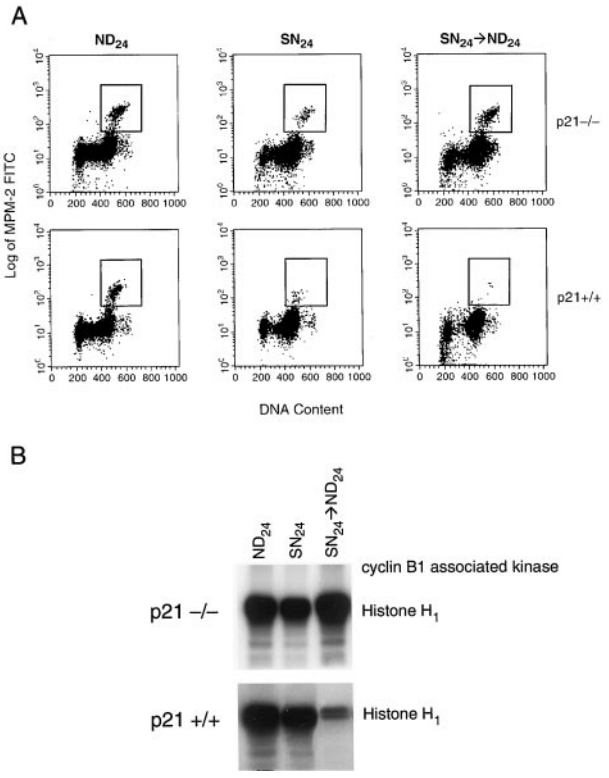

Fig. 2 Cell cycle arrest and inhibition of cyclin B1/cdc2 kinase in p21-intact and -deficient Hct116 cells to SN-38. *A*, dot plots of p21-deficient and parental Hct116 cells stained with MPM-2 antibody. The cells were treated with SN-38 for 24 h or SN-38 for 24 h, followed by removal of medium and incubation of cells in drug-free medium for 24 h. At the end of treatment, cells were fixed and stained with primary MPM-2 monoclonal antibody as described in "Materials and Methods." DNA content is represented on the *X axis*, and log of fluorescence exhibited by MPM-2-FITC conjugate is plotted on the *Y axis*. The cells staining positive for MPM-2 show increased fluorescence and were shifted above the baseline, as shown in the *boxes* in the *histograms*. *B*, cyclin B1/cdc2 kinase activity. Immunoprecipitates of cyclin B1/cdc2 from asynchronous p21-intact and -deficient Hct116 cells either untreated (ND_{24}) or treated with SN-38 for 24 h (SN_{24}) or with SN-38 for 24 h followed by drug-free medium ($SN_{24}\rightarrow ND_{24}$). We immunoprecipitated 200 μg of protein from these cells with anti-cyclin B1 and assayed the precipitates for kinase activity, using histone H1 as substrate. Experiments were repeated a minimum of three times and representative data of one experiment are presented.

We also studied the effect of SN-38 and flavopiridol on the ability of p21-intact Hct116 to form colonies. The colony formation in these cells was markedly inhibited by SN-38. Inhibition in colony formation by 60 and 98% was observed with 5 and 20 nM SN-38, respectively (Fig. 4). Exposure of cells to up to 75 nM flavopiridol alone did not inhibit colony formation. Increasing the concentration of flavopiridol to 150 and 300 nM inhibited colony formation by 50 and 95%, respectively (Fig. 4, *inset*). Cells treated sequentially with SN-38 followed by flavopiridol showed higher inhibition of colony formation at all SN-38 doses compared with SN-38 alone. Interestingly, the concurrent and reverse combination of flavopiridol followed by SN-38 showed a trend toward increased inhibition in colony formation at lower doses of SN-38, compared with single-agent

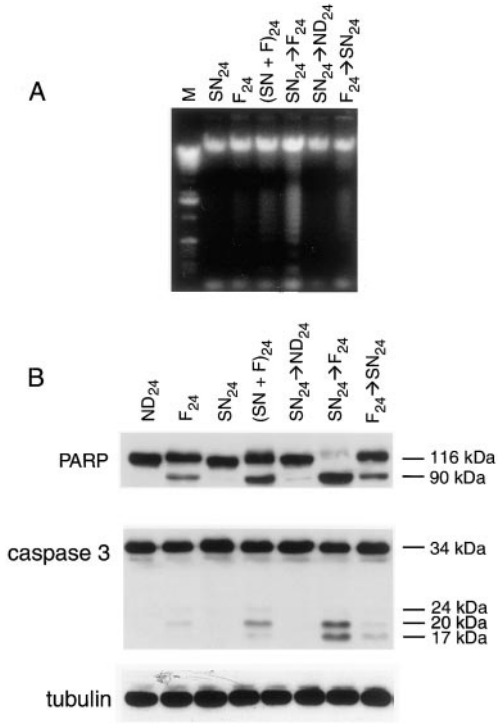

Fig. 3 Flavopiridol potentiates SN-38-induced apoptosis. *A*, gel electrophoresis analysis of DNA. p21-intact Hct116 cells were treated with different schedules of 20 nM SN-38 and 150 nM flavopiridol, and DNA was isolated as described in "Materials and Methods." Ten μg of DNA were loaded in a 1% agarose gel, and ethidium bromide-stained DNA bands were visualized under UV light. *Lane M*, molecular markers. *B*, SDS-PAGE and Western blotting with PARP and caspase-3. p21-intact Hct116 cells were treated with different schedules of 20 nM SN-38 and 150 nM flavopiridol, and protein was isolated. Fifty μg of protein were loaded on 8 or 16% (PARP and caspase-3, respectively) SDS-PAGE gels, transferred to polyvinylidene difluoride membranes, and probed with anti-PARP or -caspase-3. The equal loading of protein was verified initially by Amido black staining and later by measuring tubulin expression.

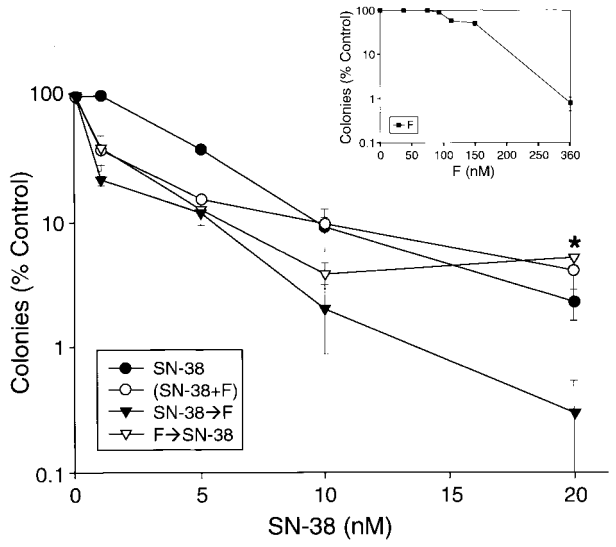

Fig. 4 Effect of SN-38 and flavopiridol on colony formation of parental Hct116 cells. Cells were treated with various concentrations of SN-38 alone (●) or with flavopiridol in three combinations: concurrent (○), sequential as SN-38 followed by flavopiridol (▼), or the two drugs given in reverse sequence (▽). *Inset*, effect of various concentrations of flavopiridol as a single agent on parental Hct116 cells.

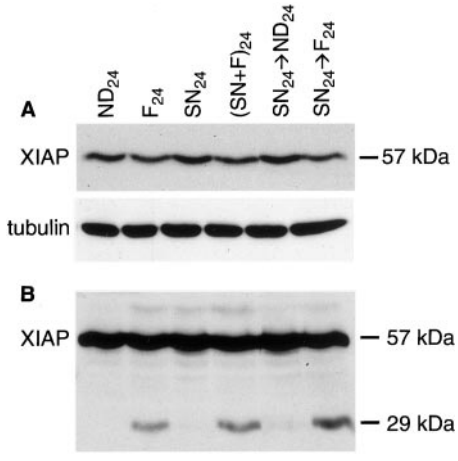

Fig. 5 Cleavage of XIAP protein during apoptosis induced by flavopiridol alone or in combination with SN-38. Asynchronous cultures of p21-intact Hct116 cells were treated with 20 nM SN-38 and 150 nM flavopiridol at the different schedules indicated, and protein was harvested. Fifty μg of protein were resolved on 16% SDS-PAGE gel and transferred to a polyvinylidene difluoride membrane. The membrane was probed with anti-XIAP monoclonal antibody. The equal loading of protein was verified initially by Amido black staining and later by tubulin expression. *A*, full-length XIAP protein is shown with shorter film exposure; *B*, full-length and cleaved product of XIAP with longer film exposure.

SN-38, and antagonism at higher SN-38 doses, as indicated by decreased inhibition of colony formation compared with SN-38 alone (Fig. 4, *). The significance of this remains unclear. Inspection of the plate for the colony assays indicated that SN-38 treated cells did not die but remained attached to the plate as permanently arrested single cells. The $SN_{24}\rightarrow F_{24}$ treatment induced cell death, and cells detached from the plate. Clonogenic assays with p21-deficient cells also showed no colony formation, and these cells completely detached from the plate with SN-38 alone (data not shown).

Molecular Regulators Associated with Enhanced Induction of Apoptosis with Sequential Treatment of SN-38 and Flavopiridol. We analyzed the molecular events of cell cycle regulation and apoptosis during SN-38 and flavopiridol treatment. The protein expression of bcl_2, bax, bad, bcl-xL, and bag was unchanged in cells treated with SN-38 followed by no drug or flavopiridol (data not shown). The inhibitor of apoptosis, XIAP, inhibits cell death via direct inhibition of caspases, including caspase-9, -7, and -3 (20–22). As shown in Fig. 5, full-length XIAP was detected as a 57-kDa protein in control untreated cells (ND_{24}). After treatment with flavopiridol (F_{24}) or a combination of SN-38 plus flavopiridol [$(SN+F)_{24}$ or $SN_{24}\rightarrow F_{24}$], the levels of full-length XIAP (57 kDa) were reduced by 20–30% (Fig. 5*A*, shorter film exposure), and a 29-kDa fragment was detected (Fig. 5*B*, longer film exposure).

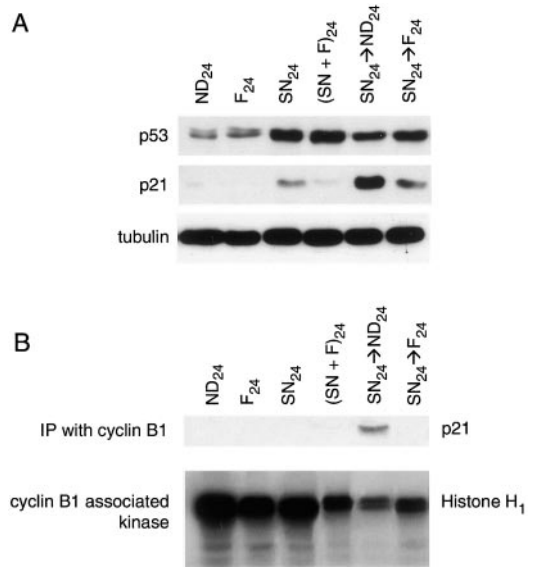

Fig. 6 p53 and p21 are induced after SN-38 treatment, and p21 (or flavopiridol) binds to cyclin B1/cdc2 complex and inhibits kinase activity. p21-intact Hct116 cells were treated with SN-38 and flavopiridol as described in the legend for Fig. 5, and protein was harvested. *A*, SDS-PAGE and Western blotting of p53 and p21. Fifty μg of protein were resolved on 15% SDS-PAGE gels and transferred to polyvinylidene difluoride membranes. The membranes were probed with mouse monoclonal p53 or p21 antibodies. The equal loading of protein was verified initially by Amido black staining and later by tubulin expression. *B*, cyclin B1/cdc2 kinase activity is inhibited after both SN-38 followed by either no drug or flavopiridol. Kinase activity was measured as in the experiment shown in Fig. 2. The experiment was repeated a minimum of three times, and representative data from one experiment are presented.

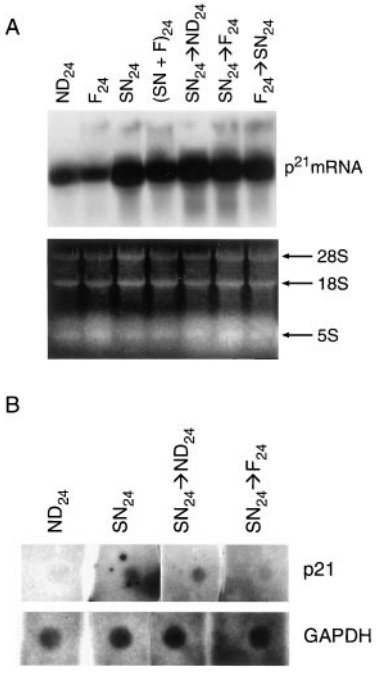

Fig. 7 Transcriptional regulation of p21 in SN-38- and flavopiridol-treated p21-intact Hct116 cells. *A*, Northern blot analysis of p21. Cells were treated with SN-38 and flavopiridol as described in the legend for Fig. 5, and total RNA was isolated as described in "Materials and Methods." Twenty μg of total RNA were denatured and separated on a 1% agarose gel. The RNA was transferred to a nylon membrane and was probed with ^{32}P-labeled p21 cDNA. Staining of the gel with ethidium bromide showed equal loading. *B*, analysis of p21 transcription by nuclear run-on assay. Cells were treated with SN-38 and flavopiridol as described in the legend for Fig. 5, and nuclear run-on assay was performed as described in "Materials and Methods." *GAPDH* was used as control gene for each treatment condition.

The intensity of the cleaved product was 4-fold higher in $SN_{24}\rightarrow F_{24}$-treated cells compared with cells treated with flavopiridol alone, suggesting higher cleavage of XIAP.

Because p21 plays an important role in cell cycle arrest and affects the sensitivity of cells to cytotoxic agents (17, 18, 23, 24), we elected to examine the protein expression of p21 in different treatment schedules in Hct116 cells. p21 is transcriptionally regulated by p53 (25). Treatment of Hct116 cells with 20 nM SN-38 for 24 h induced the protein expression of p53 and p21 by 10- and 5-fold, respectively, compared with untreated cells (Fig. 6*A*). Twenty-four h after the removal of the drug ($SN_{24}\rightarrow ND_{24}$), protein expression of p21 was further induced 5-fold. The addition of flavopiridol to SN-38-treated cells ($SN_{24}\rightarrow F_{24}$) inhibited the induction of p21 protein expression. In cells treated with flavopiridol and SN-38 concomitantly [$(SN+F)_{24}$], protein expression was lower than that in cells treated with SN-38 alone. Thus, under all treatment schedules in which flavopiridol was added and cells underwent apoptosis, p21 protein expression was down-regulated.

Because treatment with SN-38 followed by no drug resulted in inhibition of cyclin B1/cdc2 kinase activity (Fig. 2*B*) and p21 binds to cdc2 and inhibits the kinase activity (26), we analyzed the binding of p21 to cyclin B1/cdc2 in cells treated with different schedules of SN-38 and flavopiridol. The cyclin B1-associated complexes were immunoprecipitated, and Western blot analysis was performed to evaluate coimmunoprecipitated p21. As shown in Fig. 6*B*, a strong signal for p21 was observed in $SN_{24}\rightarrow ND_{24}$-treated cells. The binding of p21 to cyclin B1/cdc2 negatively regulated kinase activity, as shown by the decreased kinase activity of this complex in $SN_{24}\rightarrow ND_{24}$-treated cells (Fig. 6*B*). Flavopiridol treatment for 24 h resulted in a small decrease in kinase activity of this complex. The sequential treatment $SN_{24}\rightarrow F_{24}$, which was associated with suppression of p21 expression, also inhibited kinase activity, presumably because of direct binding of flavopiridol to cdc2.

Flavopiridol Increases the Caspase-mediated Cleavage of p21 in Sequential Therapy. To further understand the decrease in p21 protein expression in cells treated sequentially with SN-38 followed by flavopiridol, we studied the transcriptional and posttranslational changes in p21 expression in cells treated sequentially with SN-38 followed by flavopiridol. Total RNA was prepared from the Hct116 cells treated with the different schedules, and the Northern blot was probed with radiolabeled p21 cDNA. As shown in Fig. 7*A*, after 24 h of SN-38 treatment, p21 mRNA levels were increased 5-fold compared with untreated cells. The addition of flavopiridol to SN-38-treated cells did not change the mRNA levels significantly. Similar results were obtained with the nuclear run-on assays (Fig. 7*B*).

Previous studies have indicated that p21 can be degraded by the proteasome-ubiquitination pathway (27, 28) or cleaved by caspases, particularly by caspase-3 (29, 30). To investigate whether flavopiridol activated the ubiquitin-proteasome pathway for p21 degradation, p21-intact Hct116 cells were treated with the different schedules of SN-38 and flavopiridol in the presence or absence of 20 nM PS-341, a proteasome inhibitor (31). As shown in Fig. 8*A*, PS-341 stabilized the p21 protein by preventing its degradation, and treatment of cells with PS-341 for 24 h [$(PS)_{24}$] resulted in an increase in p21 protein levels compared with untreated control (ND_{24}). Addition of PS-341 together with flavopiridol to SN-38-treated cells [$SN_{24}\rightarrow(F+PS)_{24}$] prevented degradation of the p21 protein, and increased p21 protein levels were observed compared with $SN_{24}\rightarrow F_{24}$-treated cells. However, the addition of PS-341 to SN-38-treated cells ($SN_{24}\rightarrow PS_{24}$) also resulted in a similar increase in p21 protein levels (compare $SN_{24}\rightarrow ND_{24}$ and $SN_{24}\rightarrow PS_{24}$ in Fig. 8*A*). Because PS-341 also induces apoptosis and PARP cleavage in this cell line, we were unable to show reversal of apoptosis in cells treated with PS-341 in combination with SN-38 followed by flavopiridol, despite the restoration of p21 (data not shown).

We next treated the cells with SN-38 and flavopiridol in the presence of 20 μM each of the caspase-3 inhibitor z-DEVD-fmk or the pan caspase inhibitor z-VAD-fmk. As shown in Fig. 8*B*, the addition of z-DEVD-fmk or z-VAD-fmk with flavopiridol to SN-38-treated cells [$SN_{24}\rightarrow(F+z\text{-}DEVD)_{24}$ and $SN_{24}\rightarrow(F+z\text{-}VAD)_{24}$] restored the protein expression of p21. z-VAD-fmk alone or z-VAD-fmk added to SN-38-treated cells ($z\text{-}VAD_{24}$ and $SN_{24}\rightarrow z\text{-}VAD_{24}$, respectively) did not change the levels of p21, when compared, respectively, with ND_{24} and $SN_{24}\rightarrow ND_{24}$. More than 95% of PARP cleavage with SN-38 followed by flavopiridol was reversed by z-DEVD-fmk, indicating that PARP is preferentially cleaved by caspase-3 (Fig. 8*C*). The addition of z-DEVD-fmk also resulted in the disappearance of the 20- and 17-kDa cleaved fragments and the accumulation of the 24-kDa fragment of caspase-3. The pan caspase inhibitor z-VAD-fmk reversed PARP cleavage and caspase-3 activation (*e.g.*, disappearance of 24-, 20-, and 17-kDa fragments) during sequential therapy with SN-38 followed by flavopiridol [$SN_{24}\rightarrow(F+z\text{-}VAD)_{24}$; Fig. 8*C*].

Sequential Therapy with CPT-11 and Flavopiridol Augments Tumor Regression and CR in Xenografts. The clonogenic and apoptosis assays indicated that sequential treatment with SN-38 followed by flavopiridol achieved the best results. To investigate whether these *in vitro* observations are also reflected *in vivo* and to optimize the time interval between the two drugs, we established p21-intact Hct116 cells as xenografts in nude mice. Mice were treated with either each drug alone or sequentially with CPT-11 followed by flavopiridol at 4-, 7-, and 16-h intervals. As shown in Table 1 and Fig. 9, the interval between CPT-11 and flavopiridol was an important determinant of the percentage of tumor regressions in xenografts. The greatest tumor regression (the percentage of decrease in tumor volume) was observed when the interval between CPT-11 and flavopiridol was at least 7–16 h. Two weeks after the end of treatment (day 30), there was a 40 ± 25% regression of tumors in mice treated with CPT-11 alone, whereas in mice treated with CPT-11 followed by flavopiridol 7 and 16 h later, tumor regression was 86 ± 9% and 82 ± 5%,

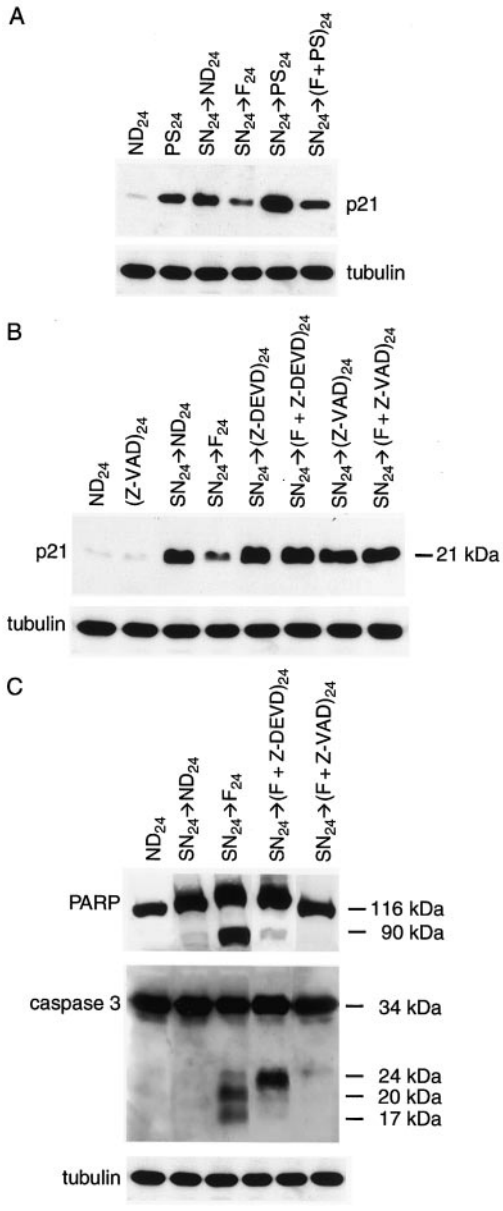

Fig. 8 Posttranslational regulation of p21 in SN-38- and flavopiridol-treated p21-intact Hct116 cells. *A*, Western blot analysis of p21 treated with SN-38/flavopiridol combination and PS-341. Cells were treated with 20 nM SN-38 followed by either no drug or flavopiridol. PS-341 (*PS*; 20 nM), a proteasome inhibitor, was added at the indicated times. *B* and *C*, p21 is cleaved by caspases. Western blot analysis of p21 (*B*) or PARP and caspase-3 (*C*). Cells were treated with SN-38 and flavopiridol, and 20 μM z-DEVD-fmk (*Z-DEVD*) or z-VAD-fmk (*Z-VAD*) was added at the indicated times. The equal loading of protein was confirmed initially by Amido black staining and later by tubulin expression.

respectively. There was no statistically significant difference in response in mice treated with CPT-11 alone and CPT-11 followed by flavopiridol after 4 h. If the interval between CPT-11 and flavopiridol was increased to 24 h, the response rate was similar to that for CPT-11 alone (data not shown). Two of 10 mice and 1 of 7 mice treated with CPT-11 followed by flavopiri-

Table 1 Tumor regression and CR in mouse xenografts treated with CPT-11 and flavopiridol

Tumors derived from p21-intact Hct116 cells were established and treated with CPT-11 alone or CPT-11 followed by flavopiridol after 4, 7, or 16 h and measured as described in "Materials and Methods."

Treatment	Tumor regression (day 30),[a] %	CR,[b] % (*n*)
CPT-11	40 ± 25	0% (0/10)
CPT-11$\xrightarrow{4\,h}$F	60 ± 17	0% (0/10)
CPT-11$\xrightarrow{7\,h}$F	86 ± 9	30% (3/10)
CPT-11$\xrightarrow{16\,h}$F	82 ± 5	29% (2/7)

[a] The tumor regression was calculated as ratio of difference between baseline and final tumor volume to the baseline volume.

[b] The CR is defined as the number of animals without tumors relative to the total number of animals in the treatment group.

dol at 7- and 16-h intervals, respectively, had no palpable tumors. We also examined the histology of any residual tissue mass remaining at the end of the treatment in different treatment groups. Despite the presence of a small palpable mass, one animal from each treatment group of CPT-11 followed by flavopiridol at 7 and 16 h showed no evidence of any tumor cells, indicating the complete pathological absence of tumor in these mice (Fig. 10). Thus, the CR rates for CPT-11 followed by flavopiridol at 7 and 16 h were 30% (3 of 10) and 29% (2 of 7), respectively. This was in contrast to CPT-11 alone or CPT-11 followed by flavopiridol at 4 h, where no CRs were found (Table 1).

The tumor growth in mice treated with CPT-11 alone or CPT-11 followed by flavopiridol was observed for at least 4–5 weeks after completion of treatment (*i.e.*, 6–7 weeks after the beginning of treatment). The growth kinetics of tumors treated with different schedules is shown in Fig. 9. Mice that received only flavopiridol showed an increase in tumor growth that was similar to that in untreated controls. After CPT-11 treatment, the tumor growth was decreased, but administration of flavopiridol after CPT-11 caused increased tumor shrinkage. The maximum tumor shrinkage, in all treatment schedules, was observed between 29 and 32 days after the start of treatment. The differences between the areas under the volume-time curves of CPT-11 alone and CPT-11 followed by flavopiridol at 7 and 16 h were statistically significant ($P = 0.0002$ and 0.0005, respectively).

Mice that were treated with only CPT-11 lost an average of 10 ± 1% of body weight, whereas mice treated with CPT-11 followed by flavopiridol at 7 and 16 h lost an average of 15 ± 2% and 11 ± 1% of body weight, respectively, suggesting that the 7-h interval was more toxic. Nevertheless, the weight loss by mice treated with CPT-11 alone and with CPT-11 followed by flavopiridol at 16 h was essentially identical. This would indicate that the difference in weight loss could not explain the significant difference in response rates for these treatment conditions. Furthermore, all mice gained weight after treatment, and the difference in the weight loss 2 weeks after completion of treatment was not different among all treatment conditions, indicating that the toxicity with the combination was temporary and within acceptable limits. None of the mice died as a result of the toxicity of either single-agent or combination therapy during the course of the experiment.

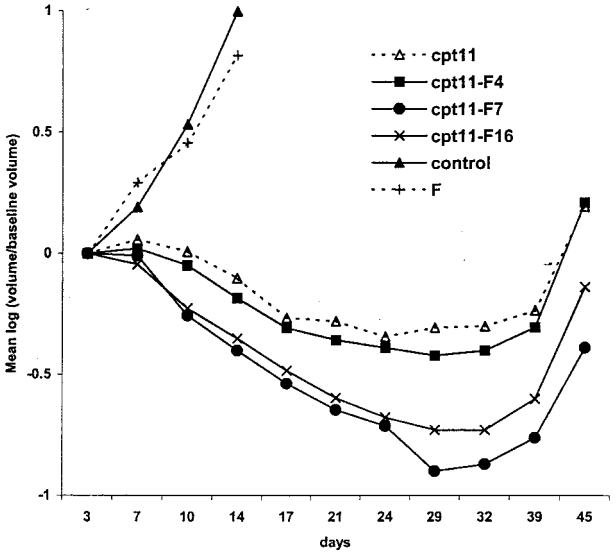

Fig. 9 Effects of CPT-11 and flavopiridol on growth of established p21-intact Hct116 xenografts in nude mice. Mice were treated with CPT-11 (*cpt11*; △) and flavopiridol alone (*F*; +) or in combination as CPT-11 followed by flavopiridol at 4 (*cpt11-F4*; ■), 7 (*cpt11-F7*; ●), and 16 h (*cpt11-F16*; ×) according to the protocol described in "Materials and Methods." Tumor volumes were measured as described in "Materials and Methods," and mean log change in volume (calculated as volume/baseline volume) was plotted against time (weeks). The control (▲) and flavopiridol-treated animals were sacrificed before 6 weeks because tumor size reached the maximum allowable limits set by Memorial Sloan Kettering Cancer Center.

DISCUSSION

In this study we show that as a single agent in Hct116 cells *in vitro*, SN-38 induces cell cycle arrest without cell death. This correlates to the absence of CRs observed *in vivo* with CPT-11 alone. The addition of flavopiridol to SN-38-treated Hct116 cells caused cell death *in vitro*, and *in vivo* this translated into greater tumor regression as well as CRs. With clonogenic assays, we observed that SN-38-treated cells remained attached to the plate as viable single cells. These cells did not form colonies because cell cycle arrest by SN-38, and this resulted in the inhibition of colony formation. However, SN-38 alone did not induce apoptosis; therefore, we did not observe PARP cleavage or caspase-3 activation. In contrast, flavopiridol added to SN-38-treated Hct116 cells induced significant apoptosis as indicated by quantitative fluorescence microscopy assays, PARP cleavage, and caspase-3 activation. We observed neither single viable cells nor colonies by clonogenic assays. In essence, flavopiridol converted the cytostatic effect of SN-38 into a cytotoxic effect such that the cells arrested in G_2 by SN-38 alone then underwent apoptosis. We believe this conversion from cell cycle arrest to cell death could account for the increase in tumor regression and CRs observed with the CPT-11-flavopiridol combination. There is certainly precedent for this concept. A previous report by Waldman *et al.* (18) indicated that cell cycle arrest by DNA-damaging agents results in single cells during clonogenic assays but that this does not result in CRs in tumor xenografts. However, the induction of apoptosis (which they report similarly as detachment of the Hct116 cells from the plate

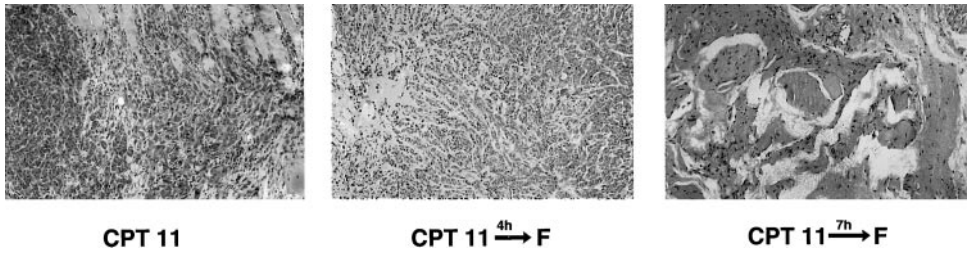

Fig. 10 Histological examination of tumors treated with CPT-11 alone and CPT-11 followed by flavopiridol at 4 or 7 h. Mice treated with CPT-11 alone and CPT-11 followed by flavopiridol at 4 h show the presence of tumor cells, whereas mice that received flavopiridol 7 h after CPT-11 show absence of any tumor cells.

with the absence of colony formation by clonogenic assays) results in higher tumor regression and CRs. Our results with CPT-11 alone and CPT-11 followed by flavopiridol in xenograft studies reflect these observations.

G_2 arrest by SN-38 is largely dependent on the checkpoint status of cells. Activation of the cyclin B1/cdc2 complex is the key regulator of G_2-M transition (32). The activation of this complex is required for G_2 cells to enter M phase. It has been shown previously that in addition to directly inhibiting the cyclin B1/cdc2 complex, p21 also inhibits Thr^{161} phosphorylation of cdc2 to enforce the G_2 DNA damage checkpoint (33). Thus, the presence of p21 (and p53) exerts a stronger G_2 arrest, as shown in parental Hct116 cells by cell cycle analysis and colony formation assays. The cell cycle changes induced by SN-38 followed by no drug and SN-38 followed by flavopiridol were similar in Hct116 cells. In cells treated sequentially with SN-38 followed by flavopiridol, although p21 protein levels were decreased, the cells were arrested in the G_2 cell cycle phase and cyclin B1/cdc2 kinase activity was also inhibited. This degree of inhibition was independent of cyclin B1 protein expression because cyclin B1 protein levels were unchanged under all treatment conditions (data not shown). The cyclin B1/cdc2 kinase activity in the kinase assays was greater than we would have anticipated in intact cells treated with SN-38 followed by flavopiridol. During immunoprecipitation, flavopiridol gets displaced from the ATP-binding site of cdc2 and competes with ATP added during the kinase assays, producing an artificial increase in kinase activity (34, 35). Although both treatment conditions (*i.e.*, SN-38 followed by no drug and SN-38 followed by flavopiridol) resulted in arrest of the cell cycle at G_2, the end results of both treatments were different (*i.e.*, SN-38 followed by no drug resulted in cell cycle arrest, whereas SN-38 followed by flavopiridol resulted in cell death). Thus, the difference between cell cycle progression and cell cycle arrest is not the mechanism by which the enhanced cytotoxicity observed with the combination of SN-38 and flavopiridol can be explained. Other mechanisms, including modulation of apoptotic pathways, are undoubtedly involved in this process.

We observed no change in the expression of proteins classically associated with apoptosis, including bcl_2, bax, bcl-xL, bad, and bag. The search for other pathways showed increased cleavage of XIAP and p21 proteins. XIAP is an inhibitor of caspases and can be cleaved by caspases during apoptosis, thus rendering cells more sensitive to cell death (21, 22). p21 is transcriptionally up-regulated after SN-38 treatment. The decrease in p21 appears to be attributable to a posttranslational effect. Both $SN_{24}\rightarrow(F+PS)_{24}$ and $SN_{24}\rightarrow PS_{24}$ produced similar increases in p21 protein levels. This would indicate that activation of the proteasome-ubiquitination cascade is a normal process for p21 degradation and that flavopiridol is not activating this process. Instead, it appears that loss of p21 is the result of cleavage of p21 by caspases, specifically by caspase-3, in sequential therapy. This was shown by the addition of z-DEVD-fmk during treatment with SN-38 followed by flavopiridol.

Caspase-3 is processed via two processing steps (36). The first step involves a single cleavage of the proenzyme to produce a p24/p12 intermediate. The 24-kDa fragment (large subunit plus prodomain) can be autocleaved to 20 kDa (large subunit plus half of the prodomain) and 17 kDa (large subunit) to produce a mature p17/p12 form of the enzyme. During SN-38/flavopiridol-induced apoptosis, we observed 24-, 20-, and 17-kDa fragments. The addition of z-DEVD-fmk together with flavopiridol to SN-38-treated cells [$SN_{24}\rightarrow(F+z\text{-}DEVD)_{24}$] inhibited the autocleavage of caspase-3 but did not prevent the activation of upstream caspases. This prevents the formation of the 20- and 17-kDa fragments by caspase-3 with a resultant accumulation of the 24-kDa fragment. The addition z-DEVD-fmk also reversed the p21 cleavage. We did observe small but consistent decreases in the transcription of p21 in $SN_{24}\rightarrow F_{24}$-treated cells. However, we believe that caspase-mediated cleavage of p21 is the dominant mechanism for the loss of p21 with $SN_{24}\rightarrow F_{24}$ sequential therapy.

Our results indicating that p21 is selectively cleaved during apoptosis are consistent with other reports and support the hypothesis that insufficient expression of p21 during DNA damage response may cause apoptosis (17–19). It has been shown that caspase-mediated cleavage of p21 into p14 is crucial in G-Rh2-induced apoptosis in SK-HEP-1 cells (37). Whether cleavage of p21 in sequential treatment with SN-38 followed by flavopiridol is simply an effect of the induction of apoptosis or whether the cleaved product is a proapoptotic element and amplifies the apoptotic cascade is unclear. Nevertheless, these studies do suggest a dual role for p21: G_2 arrest and inhibition of apoptosis. Thus, p21 may serve as a critical checkpoint target for both cell cycle arrest and apoptosis during treatment with SN-38 alone or SN-38 followed by flavopiridol, respectively. Manipulation of p21 expression by flavopiridol after DNA damage response may thus provide a novel strategy for cancer therapy. Additional studies to define the role of p21 in the

induction of apoptosis with SN-38 followed by flavopiridol are under way in our laboratory.

Because SN-38 followed by flavopiridol showed higher inhibition of colony formation and more than an additive effect when compared with single agents in apoptosis assays, we elected to test the sequential combination of CPT-11 followed by flavopiridol *in vivo*. It is intriguing that the timing of the administration of flavopiridol after CPT-11 had such a significant effect on tumor regression and CR. CPT-11 causes transient accumulation of cells in S-phase, after which cells exit and arrest at the G_2 phase of the cell cycle. Flavopiridol is a CDK inhibitor. It is possible that administration of flavopiridol too soon after CPT-11 will block cells in G_1 and prevent the cells from entering S-phase. This would then prevent the enhancement of the CPT-11 effect observed with the combination treatment. *In vitro*, when cells were treated with SN-38 for shorter periods of time (4–7 h) and then were exposed to flavopiridol for an additional 24 h, the induction of apoptosis was lower than the levels of induction observed when cells were treated with SN-38 for 24 h followed by flavopiridol for 24 h (data not shown). In contrast, *in vivo*, if flavopiridol was administered too late (*i.e.*, 24 h after CPT-11), then the percentage of tumor regression was decreased relative to that observed with CPT-11 alone. However, the *in vitro* studies were carried out in monolayers, and treatment of three-dimensional *in vivo* tumor masses may yield completely different results. This could explain the difference in the response to the timing of flavopiridol administration after CPT-11 in both the *in vitro* and *in vivo* studies.

The introduction of CPT-11 into the armamentarium of cancer drugs has lead to significant improvements in the treatment of patients with colon cancer. However, in the metastatic setting, responses to CPT-11 remain only 30% (38). As we improve on our understanding of the molecular basis for the response to camptothecin, we should be able to considerably improve on the therapeutic index. This study and others have shown that cells with defective G_2-M checkpoints are more sensitive to camptothecin. However, the challenge ahead is for the checkpoint-intact, camptothecin-resistant tumors, as represented by Hct116 parental cells. To make this agent more attractive in cancer treatment, combining it with chemotherapeutic modulators, such as flavopiridol, appears to be a logical choice. The addition of flavopiridol after SN-38 treatment appears to be necessary to activate the caspase cascade and induce apoptosis. Furthermore, we show for the first time that flavopiridol can enhance the effects of a DNA-damaging agent (*i.e.*, CPT-11) in a corresponding *in vivo* model. Therefore, flavopiridol represents a new agent for manipulating cellular mechanisms of apoptosis to shift the balance from cell cycle arrest and DNA repair to irreparable DNA damage and apoptosis. On the basis of these studies, a Phase I clinical trial of sequential CPT-11 followed by flavopiridol is now underway.

ACKNOWLEDGMENTS

We thank Dr. David S. Klimstra (Department of Pathology, Memorial Sloan Kettering Cancer Center) for histological evaluation of tumors from xenografts.

REFERENCES

1. Hartwell, L. H., and Weinert, T. A. Checkpoints: controls that ensure the order of cell cycle events. Science (Wash. DC), *246:* 629–634, 1989.

2. Hartwell, L. H., and Katsan, M. B. Cell cycle control and cancer. Science (Wash. DC), *266:* 1821–1828, 1994.

3. Paulovich, A. G., Toczyski, D. P., and Hartwell, L. H. When checkpoints fail. Cell, *88:* 315–321, 1997.

4. Hertzberg, R. P., Caranfa, M. J., and Hecht, S. On the mechanism of topoisomerase I inhibition by camptothecin: evidence for binding to an enzyme-DNA complex. Biochemistry, *28:* 4629–4638, 1989.

5. Shao, R. G., Cao, C. X., Shimizu, T., O'Connor, P. M., Kohn, K. W., Pommier, Y. Abrogation of an S-phase checkpoint and potentiation of camptothecin cytotoxicity by 7-hydroxystaurosporine (UCN-01) in human cancer cell lines, possibly influenced by p53 function. Cancer Res., *57:* 4029–4035, 1997.

6. Goldwasser, F., Shimizu, T., Jackman, J., Hoki, Y., O'Connor, P. M., Kohn, K. W., and Pommier, Y. Correlation between S and G_2 arrest and the cytotoxicity of camptothecin in human colon carcinoma cells. Cancer Res., *56:* 4430–4437, 1996.

7. Chen, A. Y., Okunieff, P., Pommier, Y., and Mitchell, J. B. Mammalian DNA topoisomerase I mediates the enhancement of radiation cytotoxicity by camptothecin derivatives. Cancer Res., *57:* 1529–1536, 1997.

8. Guichard, S., Hennebelle, I., Bugat, R., and Canal, P. Cellular interactions of 5-fluorouracil and the camptothecin analogue CPT-11 (irinotecan) in a human colorectal carcinoma cell line. Biochem. Pharmacol., *55:* 667–676, 1998.

9. Bible, K. C., Bible, R. H., Jr., Kottke, T. J., Svingen, P. A., Xu, K., Pang, Y. P., Hajdu, E., and Kaufmann, S. H. Flavopiridol binds to duplex DNA. Cancer Res., *60:* 2419–2428, 2000.

10. Motwani, M., Delohery, T. M., and Schwartz, G. K. Sequential dependent enhancement of caspase activation and apoptosis by flavopiridol on paclitaxel-treated human gastric and breast cancer cells. Clin. Cancer Res., *5:* 1876–1883, 1999.

11. Bible, K. C., and Kaufmann, S. H. Cytotoxic synergy between flavopiridol (NSC 649890, L86-8275) and various antineoplastic agents: the importance of sequence of administration. Cancer Res., *57:* 3375–3380, 1997.

12. Greenberg, M. E. Identification of newly transcribed RNA. *In:* F. M. Ausubel, R. Brent, R. E. Kingston, D. D. Moore, J. G. Seidman, J. A. Smith, and K. Struhl (eds.), Current Protocols in Molecular Biology, pp. 4.10.1–4.10.11. New York: John Wiley & Sons, Inc., 1998.

13. Dai, B., Wu, P. H., Holthuizen, E., and Singh, P. Identification of a novel cis element required for cell-density-dependent down regulation of IGF-II P3 promoter activity in CaCo2 cells. J. Biol. Chem., *276:* 6937–6944, 2000.

14. Sirotnak, F. M., DeGraw, J. I., Colwell, W. T., Piper, J. R. A new analogue of 10-deazaaminopterin with markedly enhanced curative effects against human tumor xenografts in mice. Cancer Chemother. Pharmacol., *42:* 313–318, 1998.

15. NIH. Principles of Laboratory Animal Care. NIH publication 85-23. Bethesda, MD: NIH, 1985.

16. Pratt, J. W., and Gibbons, J. D. Concepts of Nonparametric Theory, pp. 296–317. Berlin: Springer-Verlag, 1981.

17. Stewart, Z. A., Mays, D., and Pietenpol, J. A. Defective G_1-S cell cycle checkpoint function sensitizes cells to microtubule inhibitor-induced apoptosis. Cancer Res., *59:* 3831–3837, 1999.

18. Waldman, T., Zhang, Y., Dillehay, L., Yu, J., Kinzler, K., Vogelstein, B., and Williams, J. Cell cycle arrest versus cell death in cancer therapy. Nat. Med., *3:* 1034–1036, 1997.

19. Wouters, B. G., Giaccia, A. J., Denko, N. C., and Martin-Brown, J. Loss of $p21^{WAF1/CIP1}$ sensitizes tumors to radiation by an apoptosis-independent mechanism. Cancer Res., *57:* 4703–4706, 1997.

20. Deveraux, Q. L., Roy, N., Stennicke, H. R., Van Arsdale, T., Zhou, Q., Srinivasula, S. M., Alnemri, E. S., Salvesen, G. S., and Reed, J. C.

IAPs block apoptotic events induced by caspase-8 and cytochrome *c* by direct inhibition of distinct caspases. EMBO J., *17:* 2215–2223, 1998.

21. Johnson, D. E., Gastman, B. R., Wieckowski, E., Wang, G-Q., Amoscato, A., Delach, S. M., and Rabinowich, H. Inhibitor of apoptosis protein hILP undergoes caspase-mediated cleavage during T lymphocyte apoptosis. Cancer Res., *60:* 1818–1823, 2000.

22. Deveraux, Q. L., Leo, E., Stennicke, H. R., Welsh, K., Salvesen, G. S., and Reed, J. C. Cleavage of human inhibitor of apoptosis protein XIAP results in fragments with distinct specificities for caspases. EMBO J., *18:* 5242–5251, 1999.

23. Waldman, T., Lengauer, C., Kinzler, K. W., and Vogelstein, B. Uncoupling of S phase and mitosis induced by anticancer agents in cells lacking p21. Nature (Lond.), *381:* 713–716, 1996.

24. Harper, J. W., Adami, G. R., Wei, N., Keyomarsi, K., and Elledge, S. J. The p21 Cdk-interacting protein Cip1 is a potent inhibitor of G_1 cyclin-dependent kinases. Cell, *75:* 805–816, 1993.

25. El-deiry, W. S., Tokino, T., Velculescu, V. E., Levy, D. B., Parsons, R., Trent, J. M., Lin, D., Mercer, W. E., Kinzler, K. W., and Vogelstein, B. WAF1, a potential mediator of p53 tumor suppression. Cell, *75:* 817–825, 1993.

26. Bunz, F., Dutriaux, A., Lengauer, C., Waldman, T., Zhou, S., Brown, J. P., Sedivy, J. M., Kinzler, K. W., and Vogelstein, B. Requirement for p53 and p21 to sustain G_2 arrest after DNA damage. Science (Wash. DC), *282:* 1497–1501, 1998.

27. Cayrol, C., and Ducommun, B. Interaction with cyclin-dependent kinases and PCNA modulates proteosome-dependent degradation of p21. Oncogene, *12:* 2437–2444, 1998.

28. Maki, C. G., and Howley, P. M. Ubiquitination of p53 and p21 is differentially affected by ionizing and UV radiation. Mol. Cell. Biol., *17:* 355–363, 1997.

29. Zhang, Y., Fujita, N., and Tsuruo, T. Caspase-mediated cleavage of $p21^{Waf1/Cip1}$ converts cancer cells from growth arrest to undergoing apoptosis. Oncogene, *18:* 1131–1138, 1999.

30. Gervais, J. L. M., Seth, P., and Zhang, H. Cleavage of CDK inhibitor $p21^{WAF1/CIP1}$ by caspases is an early event during DNA damage-induced apoptosis. J. Biol. Chem., *273:* 19207–19212, 1998.

31. Adams, J., Palombella, V. J., Sausville, E. A., Johnson, J., Destree, A., Lazarus, D. D., Maas, J., Pien, C. S., Prakash, S., and Elliott, P. J. Proteosome inhibitors: a novel class of potent and effective antitumor agents. Cancer Res., *59:* 2615–2622, 1999.

32. Nurse, P. Universal control mechanism regulating onset of M-phase. Nature (Lond.), *344:* 503–508, 1990.

33. Smits, V. A. J., Klompmaker, R., Vallenius, T., Rijksen, G., Makela, T. P., and Medema, R. H. p21 inhibits Thr161 phosphorylation of cdc2 to enforce the G_2 DNA damage checkpoint. J. Biol. Chem., *275:* 30638–30643, 2000.

34. Losiewicz, M. D., Carlson, B. A., Kaur, G., Sauville, E. A., and Worland, P. J. Potent inhibition of cdc2 kinase activity by the flavonoid L86-8275. Biochem. Biophys. Res. Commun., *201:* 589–595, 1994.

35. Carlson, B. A., Dubay, M. M., Sausville, E. A., Brizuela, L., and Worland, P. J. Flavopiridol induces G_1 arrest with inhibition of cyclin-dependent kinase CDK2 and CDK4 in human breast carcinoma cells. Cancer Res., *56:* 2973–2978, 1996.

36. Slee, E. A., Harte, M. T., Kluck, R. M., Wolf, B. B., Casiano, C. A., Newmeyer, D. D., Wang, H-G., Reed, J. C., Nicholson, D. W., Alnemri, E. S., Green, D. R., and Martin, S. J. Ordering the cytochrome *c*-initiated caspase cascade: hierarchical activation of caspases-2, -3, -6, -7, -8 and -10 in a caspase-9-dependent manner. J. Cell Biol., *144:* 281–292, 1999.

37. Jin, Y. H., Yoo, K. J., Lee, Y. H., and Lee, S. K. Caspase 3-mediated cleavage of $p21^{WAF1/CIP1}$ associated with the cyclin A-cyclin-dependent kinase 2 complex is a prerequisite for apoptosis in SK-HEP-1 cells. J. Biol. Chem., *275:* 30256–30263, 2000.

38. Conti, J. A., Kemeny, N. E., Saltz, L. B., Huang, Y., Tong, W. P., Chou, T-C., Sun, M., Pulliam, S., and Gonzalez, C. Irinotecan is an active agent in untreated patients with metastatic colorectal cancers. J. Clin. Oncol., *14:* 709–715, 1996.

Clinical Cancer Research

Augmentation of Apoptosis and Tumor Regression by Flavopiridol in the Presence of CPT-11 in Hct116 Colon Cancer Monolayers and Xenografts

Monica Motwani, Christoph Jung, Francis M. Sirotnak, et al.

Clin Cancer Res 2001;7:4209-4219.